Verification of dose calculation algorithms in a multi-layer heterogeneous phantom using films

S. Rana[1], S. Pokharel[2]

[1]Department of Medical Physics, ProCure Proton Therapy Center, Oklahoma City, OK, USA,
[2]Department of Medical Physics, Premiere Oncology, Fort Myers, FL, USA

Abstract

The development of advanced radiation treatment techniques such as intensity modulated radiation therapy (IMRT) and volumetric intensity modulated arc therapy (VMAT) require more accurate dose calculation algorithms within the treatment planning systems (TPS) considering that the human body is composed of tissues of widely differing radiological properties and the characteristics of a therapeutic radiation treatment beam along a heterogeneous path will be different. The objective of this study was to evaluate the accuracy of 2D-isodose distributions predicted by pencil beam convolution algorithm (PBC) and anisotropic analytic algorithm (AAA) in a heterogeneous slab phantom composed of media equivalent to air, water and bone density. The measurements were done by using the films at multiple depths in the phantom for open field sizes 5 × 5 cm^2 and 10 × 10 cm^2. The results from this study indicated that the AAA had better agreement with the measurement compared to PBC for both the test field sizes at all selected depths; however, the limitation of AAA in predicting doses within and beyond low-density medium was observed, especially for a smaller field size (up to 32.7% and 34.0% for AAA and PBC, respectively). Furthermore, discrepancies up to -4.8% for AAA and -14.6% for PBC was seen in the high-density medium as well. Dose prediction errors by the AAA and PBC were more pronounced for a smaller test field size, especially in the low-density medium.

Keywords

IMRT, dose calculation algorithms, Anisotropic Analytical Algorithm (AAA), Pencil Beam Convolution (PBC), Varian's Eclipse treatment planning system

Introduction

The significant advances in external beam radiation therapy (EBRT) such as development of more accurate treatment planning systems (TPS) and linear accelerator delivery capabilities have improved the dose conformity and distributions [(1)]. The intensity modulation radiation therapy (IMRT) is an example of EBRT that combines several intensity modulated beams leading to the construction of conformal dose distributions [(2, 3)]. Most recently, a novel radiation technique called volumetric intensity modulated arc therapy (VMAT) was introduced [(4)]. The VMAT system can deliver a highly conformal radiation dose to the target by allowing the simultaneous variation of gantry rotation speed, dose rate and multiple-leaf collimators (MLC) leaf positions [(4)].

The development of these advanced radiation treatment techniques also demands more accurate dose calculation algorithms within TPS [(5)] since the human body is composed of tissues of widely differing radiological properties and the characteristics of a therapeutic radiation treatment beam along a heterogeneous path will be different. Several authors have conducted the evaluation of pencil beam convolution algorithm (PBC) and anisotropic analytic algorithm (AAA) [(6-10)], and both of these algorithms are employed within the Eclipse TPS (Varian Medical Systems, Palo Alto, CA, USA). Previous studies [(6-10)] on the accuracy of dose predictions by PBC and AAA were done by comparing the results of dose computations and measurements with ionization chamber mostly near lung/tissue interface or

Corresponding author: Suresh Rana, MS, Department of Medical Physics, ProCure Proton Therapy Center, 5901 West Memorial Road, Oklahoma City, OK 73142, USA. Email: suresh.rana@gmail.com

within lung equivalent materials or at selected depths beyond the low density medium. To our knowledge, no study has been conducted comparing the dose prediction accuracy of AAA and PBC at various depths in a multi-layer phantom with focus on film dosimetry. The motivation of this study was to investigate the dose prediction accuracy of AAA and PBC in a heterogeneous rectangular phantom composed of media equivalent to air, water and bone density. The measurements were done by using the films at multiple depths in the phantom and the evaluation of dose calculation algorithms was done by comparing the 2D-isodose distributions calculated by PBC and AAA with the 2D-isodose distributions measured by the films.

Methods

The data presented in this study were taken from a 6 Megavoltage (MV) X-ray beam of a Clinac iX linear accelerator (Varian Medical Systems, Palo Alto, CA). The open field size (FS) included in this study were 5 × 5 cm^2 and 10 × 10 cm^2. The source to surface distance (SSD) of 100 cm was used for dose computations and measurements.

Dose Calculation Algorithms

The PBC calculates the dose distribution in infinitesimally narrow pencil beams, and the dose deposition kernels are derived from the measured water data [7, 11, 12]. The corrections to each pencil beam are obtained by a correction factor to account for differences in attenuation[11, 13, 14]. The dose from the adjacent pencil beams is not considered in each calculation, which can lead to errors in determination of dose in tissues that are within areas of large inhomogeneity. The effect is a heterogeneity correction only in the beam path direction, but not in lateral direction [11-14]. In contrast, the beams in the AAA include contributions from three different photon sources: (i) bremsstrahlung photons due to interaction of electron beam with the target and do not interact with the linear accelerator head, (ii) photons scattered in the flattening filter, primary collimators and jaws, and (iii) electrons created mainly by Compton interaction in the head of the linear accelerator and air[6, 7, 8]. The total energy deposited by each beam is obtained by the convolution of the separately-modelled contributions of above mentioned three photon sources and the final dose is calculated by the superposition of the contributions from the beams [8]. The tissue heterogeneity in the AAA is handled by radiologic scaling of primary photons and photon scatter kernel scaling in lateral directions according to local electron density [6,8]. For complete understanding on the AAA and PBC, readers are advised to refer to publications by Van Esch et al. [8] and Carrasco et al. [10].

2D-Isodose Distribution Calculation

A heterogeneous slab phantom (30 × 30 cm2, 30 cm deep) was created as 3D computed tomography (CT) structure set in the Eclipse TPS (version 10.0.26) in order to simulate the experimental setup. (Fig. 1) Each phantom layer consisted of rectangular area of 30 × 30 cm^2, and the phantom layers consisting of solid-water, Styrofoam and Poly Vinyl Chloride (PVC) were assigned with CT numbers of 0, -990 and +1200, respectively. The dose calculation was performed using AAA (version 10.0.26) and PBC (version 10.0.26) for 100 Monitor Units (MUs) using identical beam setup. The calculated 2D-isodose distributions (AAA and PBC) at selected depths of the coronal plane were exported as Digital Imaging and Communications in Medicine (DICOM) files from the Eclipse TPS for subsequent 2D-isodose distribution analysis.

2D-Isodose Distribution Measurement

At selected depths in the heterogeneous rectangular slab phantom, Kodak Extended Dose Rate-2 (EDR-2) films were placed in the coronal direction and taped to the rectangular slab of solid-water, PVC tile or Styrofoam blocks. (Fig. 1) Then, by keeping identical field sizes, beam parameters and geometries that were used for dose computation by AAA and PBC in the Eclipse TPS, 300 MUs were delivered to the phantom.

2D-Isodose Distribution Analysis

Developed EDR-2 films were analyzed using RIT software (Radiological Imaging Technology, Colorado Springs, CO) and Vidar Scanner (Vidar

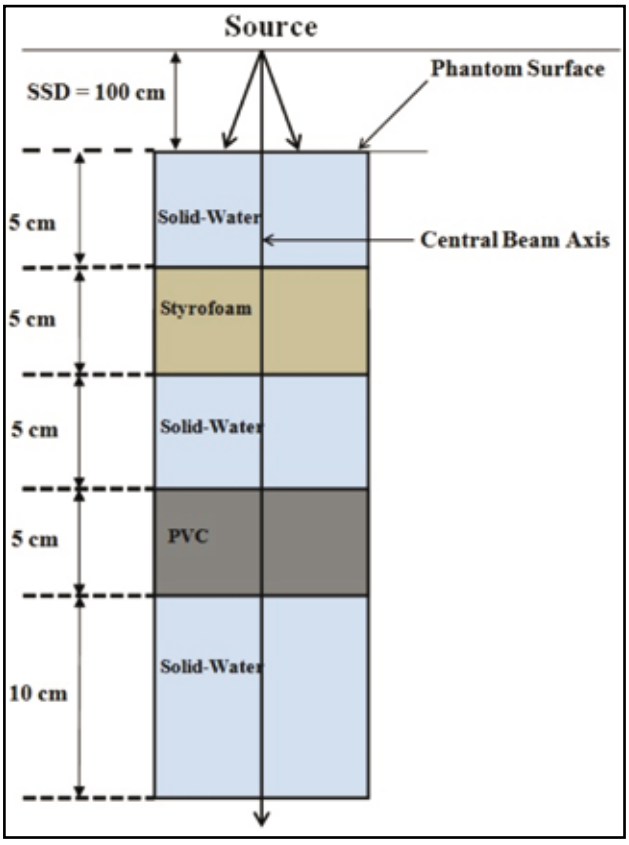

Figure Legends

Figure 1: Schematic diagram of the experimental setup for dose computations and measurements in a heterogeneous rectangular slab phantom.

Abbreviations: SSD = Source to Surface Distance, PVC = Poly Vinyl Chloride tile

Scanning System, Herndon, VA). For the isodose overlay analysis of films at selected depths, the DICOM images from the Eclipse TPS (target images) and the images from measurement (measured images) were used. The target images and measured images were normalized to their respective values obtained at the depth of 1.5 cm. After the normalization of both the target and the measured images, an isodose overlay analysis was performed for 90 % (high dose region), 50% (medium dose region) and 30% (low dose region) isodose lines.

The difference in distance between the measured (M) isodose lines and the target (T) isodose lines (AAA and PBC) was quantified. In order to do so, an isodose overlay plot was divided into 12 equal parts by drawing lines (300 apart from each other) through the center of the plot (Fig. 2). From the center of the plot, distance to the target isodose line (i.e., T1 – T12)

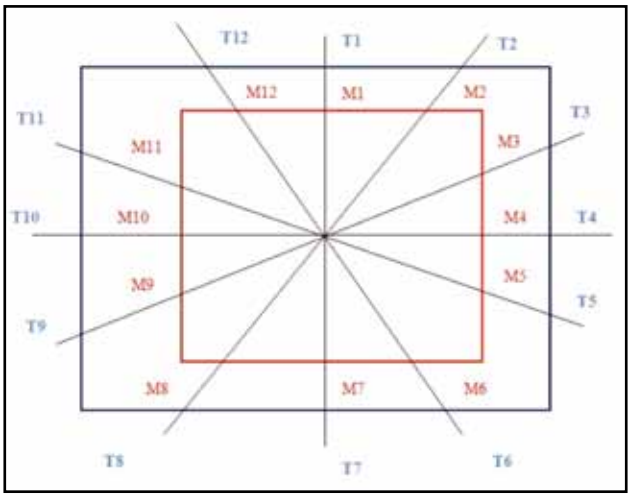

Figure 2: Isodose overlay plot analysis between target and measured isodose lines. Each isodose overlay plot (target and measured) was divided into 12 equal parts by drawing lines (300 apart from each other) through the center of the plot.

Abbreviations: T1, T2 …T12 = Target Isodose lines (blue color); M1, M2….M12 = Measured Isodose lines (red color)

and distance to measured isodose line (i.e., M1 – M12) was measured.

In Fig. 2, the red square represents the measured isodose lines (M1– M12) and the blue square represents the target isodose lines (T1 – T12). The average values, T and M were obtained at each depth for AAA and PBC by using the relationships provided below.

$$T = (1/12) \times (T1+T2+ T3+ T4+ T5+ T6+ T7+ T8+ T9+ T10+ T11+ T12)$$

$$M = (1/12) \times (M1+M2+ M3+ M4+ M5+ M6+ M7+ M8+ M9+ M10+ M11+ M12)$$

The difference (Δ) at depth, *d* was calculated using equation (I)

$$\Delta\,(d) = [(T-M)/M] \times 100 \qquad (I)$$

Results

The deviation of the target isodose lines created by AAA and PBC were compared against the measured isodose lines. Table 1 shows the isodose lines (90%, 50% and 30%) comparison at selected depths in the phantom. (Table 1)

Comparison for 90 % isodose lines (High Dose Region)

Depth (cm)	Field Size (cm^2)	PBC T (mm)	PBC M (mm)	PBC Δ (%)	AAA T (mm)	AAA M (mm)	AAA Δ (%)
90% Isodose Lines (High Dose Region)							
1.5	5 × 5	23.6	25.9	-8.8	24.3	25.2	-3.3
	10 × 10	58.0	61.2	-5.2	59.2	61.0	-2.9
50% Isodose Lines (Medium Dose Region)							
4.0	5 × 5	27.6	27.7	-0.5	27.8	27.9	-0.4
	10 × 10	59.9	60.1	-0.3	60.0	60.1	-0.2
7.0	5 × 5	31.2	23.3	34.0	27.6	20.8	32.7
	10 × 10	59.9	55.6	7.9	59.4	55.6	7.0
11.0	5 × 5	28.3	29.1	-2.6	28.7	29.1	-1.4
	10 × 10	60.5	61.1	-1.0	60.1	60.6	-0.7
14.0	5 × 5	27.7	29.0	-4.7	28.1	29.0	-3.2
	10 × 10	60.6	61.9	-2.2	61.3	62.0	-1.2
16.0	5 × 5	27.4	32.1	-14.6	30.5	32.1	-4.8
	10 × 10	60.4	61.6	-1.9	61.0	61.6	-1.0
30% Isodose Lines (Low Dose Region)							
4.0	5 × 5	29.6	29.2	1.4	29.5	29.2	1.1
	10 × 10	63.3	63.1	0.3	63.1	63.1	0.0
7.0	5 × 5	34.0	32.3	5.2	29.7	28.9	2.8
	10 × 10	62.0	61.7	0.5	61.9	61.8	0.2
11.0	5 × 5	31.1	30.7	1.4	30.9	30.6	1.0
	10 × 10	63.8	63.5	0.5	63.4	63.5	-0.1
14.0	5 × 5	31.3	31.2	0.2	31.2	31.2	0.1
	10 × 10	65.7	64.4	2.1	64.4	64.2	0.3
19.0	5 × 5	30.5	31.7	-3.9	31.1	31.7	-1.8
	10 × 10	74.6	75.2	-0.8	65.6	65.8	-0.3

Table 1: Isodose lines comparison for high, medium and low regions (from top to bottom) at selected depths in a heterogeneous rectangular slab phantom (see Figure 1) for field sizes 5 × 5 and 10 × 10 cm^2.

Abbreviations: PBC = Pencil Beam Convolution algorithm, AAA = Anisotropic Analytic Algorithm, T = Average distance from the center of isodose overlay plot to target isodose line, M = Average distance from the center of isodose overlay plot to measured isodose line,

Δ (%) = ((T-M)/M)*100

Depth 1.5 cm (Solid-water region before Styrofoam)

The 90% isodose lines comparison at depth 1.5 cm showed that the AAA was found to be in good agreement with the measurement in this high dose region. Specifically, the AAA's isodose lines deviated by -3.3% for FS 5 × 5 cm^2 and -2.9% for FS 10 × 10 cm2; whereas the deviation of PBC's isodose lines were by -8.8%

for FS 5 × 5 cm^2 and -5.2% for FS 10 × 10 cm^2 when compared to measured isodose lines.

Comparison for 50 % isodose lines (Medium Dose Region)

The 50 % isodose profile comparison was performed at selected depths in the phantom.

Depth 4 cm (solid-water region before Styrofoam)

The target isodose lines of AAA and PBC were within -1.0% of difference from the measured isodose lines for both test field sizes.

Depth 7 cm (Styrofoam)

The maximum Δ between the measured and the target isodose lines of AAA (+32.7%) and PBC (+34.0%) occurred for FS 5 × 5 cm^2 in this low-density region (i.e. Styrofoam). However, an increase in FS reduced the deviation between the target and measured isodose lines. Specifically, the difference was reduced from +32.7% to +7.0% for AAA and from +34% to +7.9% for PBC when FS was increased from 5 × 5 cm^2 to 10 × 10 cm^2.

Depth 11 cm (solid-water region in between Styrofoam and PVC)

The Δ between the measured and the target isodose lines (AAA and PBC) was by average of -1.4%, ranged from -0.7% to -2.6%.

Depth 14 cm (solid-water region in between Styrofoam and PVC)

The Δ between the measured and the AAA's isodose lines was by average of -2.2% (range, -1.2 to -3.2%); whereas the average Δ was slightly higher for PBC (-3.5%; range, -2.2 to -4.7%).

Depth 16 cm (PVC)

The isodose lines of AAA and PBC showed the deviation by -4.8% and -14.6%, respectively for FS = 5 × 5 cm^2; however, the deviation was significantly decreased for AAA (-1.0%) and PBC (-1.9%) when FS was increased to 10 × 10 cm2.

Comparison for 30 % isodose lines (Low Dose Region)

The 30 % isodose profile comparison was performed at selected depths in the phantom.

Depth 4 cm (solid-water region before Styrofoam)

The deviation of target isodose lines (AAA and PBC) were within +1.5% for FS = 5 × 5 cm^2 and less than +0.5% for FS = 10 × 10 cm^2 from the measured isodose lines.

Depth 7 cm (Styrofoam)

The target isodose lines of AAA and PBC had the difference of +2.8% and +5.2%, respectively for FS 5 × 5 cm^2, whereas the difference reduced to 0.2% and 0.5%, respectively for FS 10 × 10 cm2.

Depth 11 cm (solid-water region in between Styrofoam and PVC)

The Δ between the measured and the target isodose lines (AAA and PBC) was by average of +0.7%, ranged from -0.1% to +1.4%.

Depth 14 cm (solid-water region in between Styrofoam and PVC)

The Δ between the measured and the AAA's isodose lines was within +0.5% for both test field sizes; whereas the Δ for PBC ranged from +0.2% (FS = 5 × 5 cm^2) to +2.1% (FS = 10 × 10 cm2).

Depth 19 cm (PVC)

The isodose lines of AAA and PBC showed the difference by -1.8% and -3.9%, respectively for FS = 3 × 3 cm^2. The difference was reduced for AAA (-0.3%) and PBC (-0.8%) when FS was increased to 10 × 10 cm^2.

Discussion

In this study, dose calculation accuracy of AAA and PBC has been evaluated by comparing the calculated and measured 2D-isodose distributions at multiple depths in a heterogeneous slab phantom. The 2D-isodose distribution analysis was done at high (90% isodose), medium (50% isodose) and low (30% isodose) dose regions. Our results indicated that the measured isodose lines had the least deviation from the AAA's isodose lines when compared against the isodose lines of PBC at all selected depths, and this was true for both FS

used in this study. Although the AAA had better agreement with the measurement compared to PBC, the results showed the limitation of AAA in predicting doses within and beyond low-density medium (Styrofoam), especially for a smaller field size. Furthermore, discrepancies up to -4.8% for AAA and -14.6% for PBC was seen in the high-density (PVC) medium as well. Media of different density causes electronic disequilibrium at and near their heterogeneity interface as the lateral range of secondary electrons becomes longer than the width of the small field segments [5, 15]. Thus, dose calculation algorithms must have tissue heterogeneity corrections that will account accurately for the electron transport near the tissue heterogeneity interface.

Previous studies[6, 7, 8] have also shown the limited dose prediction accuracy of AAA and PBC in the heterogeneous media. Gray et al [7] reported that the dose overestimation by AAA and PBC is greater than 2.5% beyond a large air gap. Robinson et al [6] investigated the central axis depth dose beyond heterogeneity layer of 2 - 10 cm air gap, and reported that the AAA tends to overestimate dose by 3 - 7%. In another study by Van Esch et al [8] showed that the AAA overestimated the dose by up to 7% beyond the cork slab. The dose prediction errors reported in previous studies as well as in our study may also be due to the approximations employed within dose calculation algorithms when media of different densities are involved. When a photon beam traverses low-density medium (Styrofoam in this study), loss of lateral scatter radiation occurs, and the dose calculation algorithm must be able to account the lateral scatter contribution to the measurement points within and beyond the low-density medium. Furthermore, photon beam is hardened when it traverses high density medium (PVC) due to removal of low energy photons from the beam, and this causes increased number of ionizations in the medium leading to increase in the dose absorption downstream. Thus, more accurate photon beam modeling for lateral scatter, beam hardening as well as primary beam attenuation is essential to avoid the dose overestimation or underestimation in the clinical practice. The impact of different thickness of air or bone equivalent materials on the dose prediction accuracy of AAA and PBC would be an interesting topic for future studies. In summary, the results of this study showed that the measurements had better agreement with the AAA compared to PBC. Dose prediction errors by the AAA and PBC were more pronounced for a smaller test field size, especially in the low-density medium.

References

1. Webb S. Intensity-modulated radiation therapy. Bristol: Institute of Physics Publishing 2000.
2. Guerrero Urbano MT, Nutting CM. Clinical use of intensity-modulated radiotherapy: part I. Br J Radiol 2004; 77:88–96.
3. Veldeman L, Madani I, Hulstaert F, et al. Evidence behind the use of intensity-modulated radiotherapy: a systematic review of comparative clinical studies. Lancet Oncol 2008; 9:367–375.
4. Otto K. Volumetric modulated arc therapy: IMRT in a single gantry arc. Med Phys 2008; 35:310–317.
5. Das IJ, Ding GX, Ahnesjö A. Small fields: Nnonequilibrium radiation dosimetry. Med Phys 2008; 35(1):206–15.
6. Robinson D. Inhomogeneity correction and the analytic anisotropic algorithm. J Appl Clin Med Phys 2008; 9(2):2786.
7. Gray A, Oliver LD, Johnston PN. The accuracy of the pencil beam convolution and anisotropic analytical algorithms in predicting the dose effects due to attenuation from immobilization devices and large air gaps. Med Phys 2009; 36(7):3181-3191.
8. Van Esch A, Tillikainen L, Pyykkonen, et al. Testing of the analytical anisotropic algorithm for photon dose calculation. Med Phys 2006; 33(11):4130-4148.
9. Ding W, Johnston P, Wong T, et al. Investigation of photon beam models in heterogeneous media of modern radiotherapy. Australas Phys Eng Sci Med 2004; 27: 39–-48.

10. Carrasco P, Jornet N, Duch M, et al. Comparison of dose calculation algorithms in phantoms with lung equivalent heterogeneities under conditions of lateral electronic disequilibrium. Med Phys 2004; 31: 2899–2911.

11. Storchi P, Van Battum L, Woudstra E. Calculation of a pencil beam kernel from measured photon beam data. Phys Med Biol 1999; 44: 2917–2928.

12. Mohan R, Chui C, Lidofsky L. Differential pencil beam dose computation model for photons. Med Phys 1986; 13: 64-73.

13. Hurkmans C, Knoos T, Nilsson P, et al. Limitations of a Pencil Beam approach to photon dose calculations in the head and neck region. Radiother Oncol 1995; 37:74–80.

14. Sontag M, Cunningham J. Corrections to absorbed dose calculations for tissue inhomogeneities. Med Phys 1977; 4: 431-436.

15. Knöös T, Wieslander E, Cozzi L, Brink C, Fogliata A, Albers D, Nyström H, Lassen S. Comparison of dose calculation algorithms for treatment planning in external photon beam therapy for clinical situations. Phys Med Biol 2006; 51:5785-807

16. Dutreix J, Dutreix A, Tubiana M. Electronic equilibrium and transition stages. Phys Med Biol 1965; 10: 177–190.